JOURNAL OF INTERDISCIPLINARY
METHODOLOGIES AND ISSUES
IN SCIENCE

When and how to fallow: first steps towards banana crop yield improvement through optimal and sustainable control of a soilborne pest

Israël TANKAM CHEDJOU[*1], **Frédéric GROGNARD**[2], **Jean Jules TEWA**[1,3], **Suzanne TOUZEAU**[2,4]

[1]Department of Mathematics, University of Yaoundé I, Cameroon
[2]Université Côte d'Azur, Inria, INRAE, CNRS, Sorbonne Université, BIOCORE, France
[3]National Advanced School of Engineering, University of Yaounde I, Cameroon
[4]Université Côte d'Azur, INRAE, CNRS, ISA, France

*Corresponding author: israeltankam@gmail.com

DOI: 10.18713/JIMIS-120221-8-4
Submitted: 25 July 2020 - Published: 12 February 2021
Volume: **8** - Year: **2021**
Issue: **Digital agriculture in Africa**
Editors: *Mathieu Roche, Pascal Bonnet, Hélène Kirchner*

Abstract

The main hindrance to banana crop yields is the burrowing nematode *Radopholus similis*, a microscopic worm that feeds and develops in plant roots. *R. similis* is an obligatory parasite that fortunately resists badly in the absence of its host. Hence, the deployment of fallows is an efficient way to keep its populations low enough in the soil to have good economic returns on banana bunches. The banana plant is a perennial plant which reproduces itself by budding from its roots, but after a fallow period, a nematode-free sucker needs to be planted to provide for the next cropping season. Fallow is a recommended cropping practice to reduce nematode infestation, but it comes at the cost of nematode-free suckers. Moreover, fallows reduce the time devoted to growing bananas on a given time horizon and may reduce the total yield. A trade-off should then be found between fallow deployment to reduce pest infestation and economic returns. The questions that emerge are when to leave room for the natural reproduction of the banana plant, and when to deploy the fallow? How long to deploy the fallow if applicable? On the basis of mathematical models this paper attempts to answer the questions.

Keywords

yield optimization; semi-discrete model; epidemiological model; pest management; burrowing nematode

---

I INTRODUCTION

Since the human population rapidly grows, food security is becoming a major challenge as it is estimated that about nine billion people will need to be fed in 2050 [Bahar *et al.* (2020)].

This challenge is even more crucial with regard to staple foods. Bananas and cooking bananas, usually called "plantains", are important staple foods in the world along with rice, wheat and maize, and one of the most popular fruits in the world [Food and Agriculture Organization of the United Nations (FAO) (2020); Plowright *et al.* (2013)]. Collectively called "banana", they are grown in more than 135 countries, are found in most tropical and subtropical regions of the world and occupy about 0.1 percent of the world agricultural surface [Liu (2008)]. Available data indicate that between 2000 and 2017, global production of bananas grew at a compound annual rate of 3.2 percent, reaching a record of 114 million tonnes in 2017, up from around 67 million tonnes in 2000 [Food and Agriculture Organization of the United Nations (FAO) (2020)]. Plantain is a major food and cash crop in West and Central Africa and is of great importance in Cameroon [Temple *et al.* (2006)]. It involves many stakeholders (more than 600 000 producers and around 40 000 tradesmen) and contributes to 2% of the gross domestic product [Efanden *et al.* (2005)].

As for other staple foods, banana crop yields are hampered by several pests. One of the most important threats is the burrowing nematode *Radopholus similis* which is the most significant parasitic nematode of the banana and plantain plants in the world [Sarah (1993)]. Its damages reduce the production and can lead to the toppling of the plant. Unfortunately, the control of *R. similis* still requires pesticides which are not always very effective and pollute the environment. Because this method of control is not sustainable, it has been banned in some countries [Gowen (1997)], and some agricultural practices like fallow are preferred [Chabrier and Quénéhervé (2003); Chabrier *et al.* (2005, 2010)].

Because of the large number of factors and the complexity of interactions between plants and pests, mathematical models are invaluable tools to synthesize knowledge on pests and to quantify the effects of cropping systems on pest dynamics. Therefore, improving the efficacy of sustainable agricultural practices, especially for soilborne pest control, relies more and more on mathematical modelling. In the early 90s, Gilligan (1990, 1995) proposed some models that described the dynamics of soilborne pathogens. These models were generalized by Gubbins *et al.* (2000). Madden and Van Den Bosch (2002) and Mailleret *et al.* (2011) introduced semi-discrete formalisms to account for multi-seasonality in the dynamics of soilborne pests in interaction with host plants. In line with the latter, we proposed in 2020 a multi-seasonal model for the dynamics of the soilborne pest *R. similis* taking into account the particularities of banana crops [Tankam-Chedjou *et al.* (2020)]. We further describe optimal fallow deployments in this model, in order to improve banana crop yields over a fixed time horizon [Tankam-Chedjou *et al.* (2021)].

Optimization of fallow deployment strategies for soilborne pest control in the literature is rare and rather unsophisticated. Van den Berg and Rossing (2005) designed optimal rotation strategies between host and fallows over several yearly cycles in order to manage crop losses due to the root lesion nematode *Pratylenchus penetrans*. These strategies consist of deciding whether or not to deploy a one-year fallow. They thus concluded, on the basis of their statistical model, when to deploy a fallow but its length was fixed. Other models, also worthy of interest, sought for optimal rotation strategies between good and bad hosts [Taylor and Rodrìguez-Kábana (1999)] or different cultivars of the same host species [Van Den Berg *et al.* (2006); Van den Berg *et al.* (2012); Nilusmas *et al.* (2020)]. Although they do not deal with fallow deployment, the principle of reducing pathogen populations in the absence of a good host remains the same, and good lessons can be learned from these latter models.

The main problem with our latter optimization [Tankam-Chedjou *et al.* (2021)] is that after each banana cropping season a fallow period, even a short one, is introduced. As a result, to start a new cropping season, banana growers cannot rely on the natural reproduction of banana plants by budding from their roots, but need to buy and plant banana suckers (vitroplants). Buying healthy vitroplants comes at a significant cost. Moreover, fallows reduce the time devoted to growing bananas on a given time horizon and may reduce the total yield. Hence, systematic fallow deployment may not be optimal. The purpose of this paper is therefore to determine when to deploy a fallow and how long it should last, to maximize the profit on a fixed time horizon.

In Section II, we briefly describe the biology of banana plants and *R. similis* in order to understand their interactions, in particular with regard to the differences in banana reproduction means we addressed in this introduction. In Section III, we remind the multi-seasonal framework and the model we built in Tankam-Chedjou *et al.* (2020), as well as some long-term dynamic results. We then briefly present the optimization results with systematic fallow deployment of Tankam-Chedjou *et al.* (2021) in Section IV. Finally, we present in Section V more sophisticated fallow deployment strategies which are the main purpose of this paper, as well as the first optimization results. We end with a great conclusion in Section VI.

II BIOLOGICAL BACKGROUND

Banana is a perennial herbaceous plant widely cultivated in tropical and subtropical regions. As a non-seasonal crop, bananas are available fresh year-round. It is a perennial crop because it produces succeeding generations of crops. The plant reproduces asexually by producing suckers which are outgrowths of the vegetative buds set on the rhizome during leaf formation and which share their parent rhizome during their early development [Eckstein and Robinson (1999)]. Hence, if the parent plant is infested, so are the suckers [Eckstein and Robinson (1999); Duncan *et al.* (1990)]. In commercial plantations, one sucker is usually selected to grow out and regenerate the plant [Robinson and Saúco (2010)]. In order to avoid the direct transmission of pests from parent plant to sucker, an alternative reproduction method can be implemented: after the harvest of the bunch, the banana plant is uprooted and a new healthy vitroplant is planted, usually after the fallow [Chabrier and Quénéhervé (2003)]. The banana plant produces roots continuously until the flowering [Beugnon and Champion (1966)]; then the plant growth concentrates on the shoots and fruits. At the end of the cropping season, the banana bunch is harvested and the plant is either cut down, or it dies naturally [Robinson and Saúco (2010)]. The roots that are not involved in the growth of the sucker quickly lose their freshness by senescence [Moreau and Le Bourdelles (1963)].

Like most nematodes in the *Pratylenchidae* family, the burrowing nematode *Radopholus similis* is an obligate parasite that feeds on banana roots. Rarely found in the soil, this nematode is mainly found in roots and rhizomes in which it penetrates, travels and feeds [Araya and Centeno (1995)]. When it infects functional roots, *R. similis* directly destroys cells and also facilitates the entry and development of saprophagous and secondary parasite [Blake (1966); Loridat (1989)] inducing root necrosis [Hugon and Picard (1988)]. It mostly reproduces sexually, even though females can use parthenogenesis to self-fertilize if males are lacking [Kaplan and Opperman (2000)]. Fertilized females lay about five eggs daily in root necrotic areas, for 2 weeks [Marin *et al.* (1998)]. From these eggs, young larvae emerge, which can either remain in the root and burrow to feed on fresh tissues, or end up in the soil in search of new roots to colonize [Hugon and Picard (1988)].

III PLANT-NEMATODE INTERACTIONS IN A MULTI-SEASONAL CONTEXT

In this section, we present the earlier modelling work which underlies the main optimization results of this article. This work is more detailed in Tankam-Chedjou *et al.* (2020).

3.1 Multi-seasonal dynamic model

Based on the biological background of the previous section, the basic model describes the root-nematodes interactions of a single plant during a cropping season. It is composed of a compartment P for the population of free nematodes in the soil, a compartment X for the population of infesting nematodes in the roots and a compartment S for fresh roots biomass. Let D denote the duration of a cropping season and d the duration between the beginning of the season and the flowering of the plant. The dynamics of the interaction between nematodes and plant roots during the $(k+1)$-th cropping seasons is given by the following equation for $t \in (t_k, t_k + D]$:

$$\begin{cases} \dot{P} = -\beta PS + \alpha a(1-\gamma)\dfrac{SX}{S+\Delta} - \omega P, \\ \dot{S} = \rho(t)S\Big(1 - \dfrac{S}{K}\Big) - a\dfrac{SX}{S+\Delta}, \\ \dot{X} = \beta PS + \alpha a\gamma\dfrac{SX}{S+\Delta} - \mu X, \end{cases} \tag{1}$$

with:

$$\rho(t) = \begin{cases} \rho & \text{for } t \in (t_k, t_k + d], \\ 0 & \text{for } t \in (t_k + d, t_k + D], \end{cases}$$

where β is the infestation rate of free nematodes, a is the consumption rate of fresh roots by free nematodes, Δ is the half-saturation constant of the consumption term, α is the conversion rate of ingested roots, γ is a proportion of nematodes that remains inside the roots, μ and ω are mortality rates, ρ is the growth rate and K the carrying capacity of the roots.

At the end of this cropping season, i.e. at $t = t_k + D$, two cases may arise:

(i) A sucker grows from the parent plant. A proportion q of the parent plant roots turns into the sucker roots and, assuming a homogeneous distribution of nematodes in the roots, the sucker bears the same proportion q of infesting nematodes inherited from the parent plant. At harvest, the parent plant is cut down and the sucker is left to grow. We assume that the (1-q) proportion of parent plant roots that do not turn into sucker roots instantaneously lose their freshness and release their nematodes to the soil. We hence obtain the following switching rule between seasons:

$$\begin{cases} P(t_{k+1}^+) = P(t_k) + (1-q)X(t_k), \\ S(t_{k+1}^+) = qS(t_k), \\ X(t_{k+1}^+) = qX(t_k). \end{cases} \tag{2}$$

In this case, $t_{k+1} = t_k + D$.

(ii) The plant is uprooted, a fallow is introduced, and then a pest-free vitroplant is planted. We assume that a fraction r of infesting nematodes remains in the soil in addition to the free nematodes inherited from the cropping season, so $P(t_k + D^+) = P(t_k + D) + rX(t_k + D)$. Free nematodes then undergo an exponential decay [Chabrier *et al.* (2010)] at rate ω during a fallow of length τ_{k+1} until the beginning t_{k+1}^+ of the next cropping season, when a healthy vitroplant of biomass S_0 is planted. We therefore have the following switching rule between seasons:

$$\begin{cases} P(t_{k+1}^+) = \Big(P(t_k+D) + rX(t_k+D)\Big)e^{-\omega\,\tau_{k+1}}, \\ S(t_{k+1}^+) = S_0, \\ X(t_{k+1}^+) = 0, \end{cases} \tag{3}$$

In this case, $t_{k+1} = t_k + D + \tau_{K+1}$.

The diagram in Figure 1 summarizes the multi-seasonal dynamics described in equations (1-3).

3.2 Parameters and reproduction numbers

3.2.1 Parameter values

We first give in Table 1 the numerical values of the parameters of models (1,2) and (1,3). For parameters that do not clearly appear in the literature, some appropriate measures were taken to set them to realistic values [Tankam-Chedjou *et al.* (2020)]. See Appendix A for details. Initial conditions are chosen as follows: at $t_0^+ = 0^+$, we assume that a healthy sucker of biomass S_0 is planted and that the soil is infested by P_0 nematodes; $S(0^+) = S_0$, $X(0^+) = 0$, $P(0^+) = P_0$.

Param.	Description	Value
d	Root growth duration	210 days
D	Cropping season duration	330 days
β	Infestation rate	10^{-1}
K	Maximum root biomass	150 g
ρ	Root growth rate	0.025 day^{-1}
ω	Mortality rate of free pests	0.0495 day^{-1}
μ	Mortality rate of infesting pests	0.045
a	Consumption rate	2.10^{-4} g.day^{-1}
α	Conversion rate of ingested roots	400 g^{-1}
Δ	Half-saturation constant	60 g
γ	Proportion of pests laid inside	0.5
q	Proportion of roots forming the new sucker during natural reproduction	$1/3$
r	Proportion of pests released in soil after uprooting	5%
S_0	Initial root biomass	60 g
P_0	Initial soil infestation	100

Table 1: Parameter values (see Tankam-Chedjou *et al.* (2020) and references therein for more details).

The basic reproduction number R_0 is the number of free pests at the beginning of a season produced by a single free pest at the beginning of the previous season, in a pest-free context [Mailleret *et al.* (2011)]. To compute this number, we studied the season-to-season discrete dynamics of the total pest population in the neighbourhood of the pest free solution. Details are given in Tankam-Chedjou *et al.* (2020). With the parameter values of Table 1, we obtain $R_0 = 97.7$ for system (1,2) which implements vegetative reproduction. Without control, a single nematode therefore produces a huge number of nematodes, which persist with an oscillating population [Quénéhervé (1989); Sarah (1986); Tankam-Chedjou *et al.* (2020)].

The effective reproduction number R corresponds to the basic reproduction number when computed on a system with control measures [Thompson *et al.* (2019), such as system (1,3) with fal-

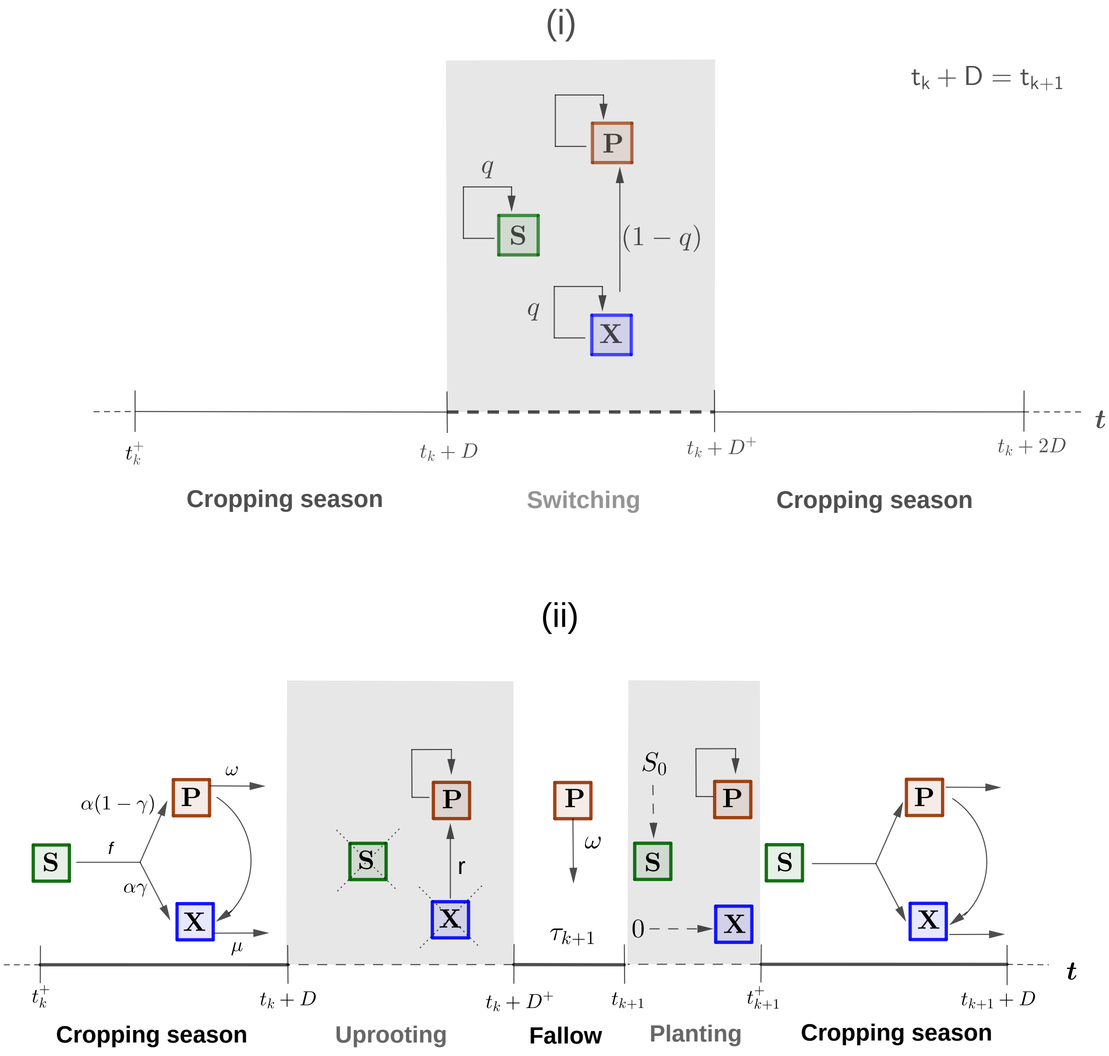

Figure 1: Schematic representation of the multi-seasonal plant-nematode dynamics with (i) natural vegetative reproduction or (ii) uprooting and pest-free vitroplant planting. Interactions between fresh roots (S), free nematodes (P), and infesting nematodes (X) during the cropping seasons correspond to Eq. (1). Switching between the cropping seasons corresponds either to: (i) Eq. (2) when no control measure is implemented and a sucker grows from the parent plant; or (ii) Eq. (3) when a fallow of duration τ_{k+1} is introduced between the parent plant uprooting and the planting of a pest-free vitroplant. On the time axis, plain lines represent the continuous course of time, whereas dotted lines and grey backgrounds represent discrete times and phenomena (parent plant cutting or uprooting, vitroplant planting). Boxes represent model variables, plain arrows population flows, dashed arrows planting and crossed-out boxes uprooting.

Fallow duration τ (days)	Effective reproduction number $\mathcal{R}$	Nematode population behaviour
83.3	0.1	decline
38.9	0.9	decline
36.8	1	
34.9	1.1	survival
0	6.2	survival

Table 2: Effective reproduction number of model (1,3) with constant fallows for different fallow durations τ. The threshold duration around which nematodes decline or survive is $\tau = 36.8$ days, corresponding to $\mathcal{R} = 1$. The highest effective reproduction number occurs without fallows ($\tau = 0$) but is much lower than the basic reproduction number of model (1,2) because of the uprooting.

lows. Its computation is similar to the basic reproduction number and also detailed in Tankam-Chedjou *et al.* (2020). With the parameter values of Table 1 and constant fallows ($\tau_k = \tau$), R can take several values, according to the fallow duration τ, that are summarized in Table 2.

IV OPTIMIZING SYSTEMATIC FALLOW DEPLOYMENT

In this section, we summarize the optimization results obtained in Tankam-Chedjou *et al.* (2021). The aim is to determine an the optimal lengths of fallow periods τ_i in model (1,3) that maximize the multi-seasonal crop profit.

4.1 Crop yield and optimization problem

4.1.1 Crop yield and profit

Banana roots are responsible for the absorption of nutrients, which are allocated to the growth of the bunch when the bunch effectively appears, i.e. after the flowering of the plant. Hence, the yield is related to the biomass of fresh roots during the bunch's growth periods $(t_k + d, t_k + D]$. So the yield of the $(k+1)$-th is given by the following formula [Tankam-Chedjou *et al.* (2021)]:

$$Y_k = m \int_{t_k+d}^{t_k+D} S(t)\, dt, \tag{4}$$

where m is the monetary root to yield conversion rate.

Assuming a fixed cost c for vitroplants [Ngo-Samnick (2011)], we obtain the following seasonal profit:

$$R_k = m \int_{t_k+d}^{t_k+D} S(t)\, dt - c. \tag{5}$$

When n fallows are deployed, the cumulated multi-seasonal profit of the $(n + 1)$ cropping seasons is then:

$$R(\tau_1, \dots, \tau_n) = \sum_{k=0}^{n} R_k \tag{6}$$

4.1.2 *Optimization problem*

From the switching rule (3), as the nematode population decreases during a fallow period, it seems reasonable to increase the fallow durations in order to reduce the pest population and therefore increase the yield. However, on a fixed and finite time horizon, increasing the fallow durations may reduce the number of cropping seasons and hence the multi-seasonal profit. The optimization problem is therefore to find a sequence of fallow durations that maximizes the overall yield over a given time horizon. For the problem to be relevant, the time horizon should allow to deploy at least one fallow period, so we assume from now on that $T_{max} > 2D$.

The problem can be stated as follows:

Problem IV.1:
Find a sequence of fallow durations $(\tau_1^*, \dots, \tau_n^*)$, with $n \geq 1$, that maximizes R defined in equation (6) on a fixed horizon T_{max}.

Remark IV.1:
Constraints may be added to the fallow durations: that may be bounded or even constant over time.

4.2 Optimal fallow deployment

4.2.1 *Theoretical results*

Our first main finding in Tankam-Chedjou *et al.* (2021) was the following lemma:

Lemma IV.1:
Under "realistic assumptions" detailed in Tankam-Chedjou *et al.* (2021), if Problem IV.1 admits a solution, then it belongs to one of the n-simplexes:

$$A^n = \big\{(\tau_1, \dots, \tau_n) : \sum \tau_k = T_{max} - (n+1)D\big\}, \tag{7}$$

with $n = 1, ..., n_{max} \equiv \left\lfloor \frac{T_{max}}{D} \right\rfloor - 1$.

This means that the last harvest needs to occur at T_{max}. We then proved that Problem IV.1 admitted a solution.

4.2.2 *Numerical resolution*

To solve Problem IV.1, we proceeded as follows. For each $n \leq n_{max}$, we seek the n-optimal fallow deployment $(\tau_1^*, \dots, \tau_2^*)$. For $n = 1$ the solution is trivial; for $n > 1$, the n-optimum is computed using an adaptive random search (ARS) algorithm, adapted to simplex A^n. As the function R defined in Equation 6 is discontinuous and not convex, gradient-based or hessian-based optimizations can quickly get stuck in the attraction region of a local maximizer. The ARS is a global search algorithm that manages to escape from strictly local maximizers and leads towards a global one. Moreover, it performs well (convergence is fairly quick), even for ill-structured global optimization problems. The optimal fallow deployment corresponds to the n-optimum that yields the highest profit R.

4.2.3 A case study

We solved Problem IV.1 with parameters in Tables 1 and 3. Results are shown in Figure 2(a). As the optimal fallow distribution is very irregular, with first very long fallows and at the end no fallows at all, we introduced an upper bound on the fallows. The optimal distribution of bounded fallows is illustrated in Figure 2(b). It seems more realistic to implement than the unconstrained optimal strategy and only insures a slight profit loss.

Param.	Description	Value
c	cost of a vitroplant	230 XAF $^{(1)}$
m	monetary root to yield conversion rate	0.3 XAF.g^{-1}.day^{-1}
T_{max}	Time horizon	4000 days

$^{(1)}$ XAF is the currency of Cameroon (1 XAF = 1.52×10^{-3} €).

Table 3: Parameter values for profit optimization (see Tankam-Chedjou *et al.* (2021) and references therein for more details).

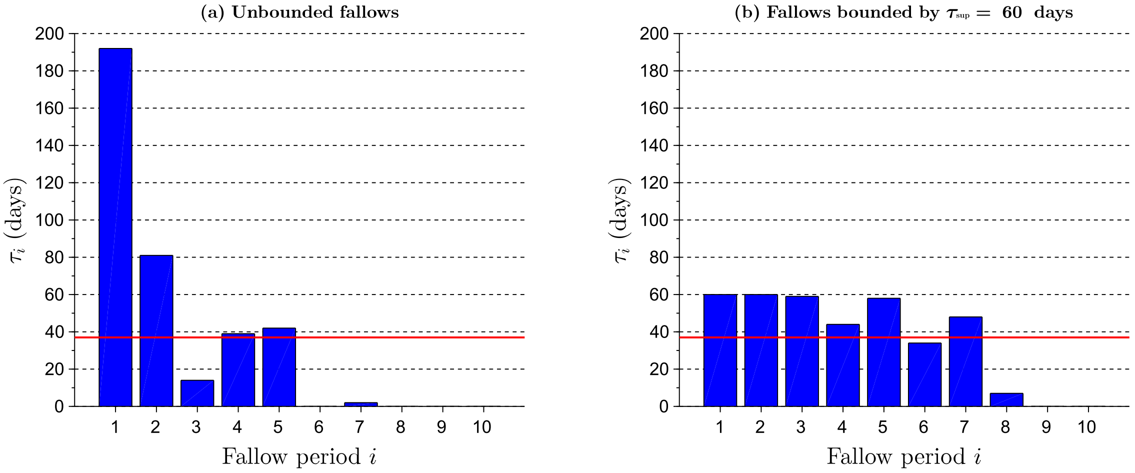

Figure 2: Optimal distribution of fallow periods with (a) unconstrained and (b) bounded fallows, solutions of Problem IV.1. The maximal profit is obtained in both cases for 11 cropping seasons and 10 fallows. Optimal fallow durations and resulting profits are: (a) : $\tau^* = (192, 81, 14, 39, 42, 0, 2, 0, 0, 0)$ and R = 54,530 XAF (83.2 €); (b) : $\tau^* = (60, 60, 59, 44, 58, 34, 48, 7, 0, 0)$ and $R = 54400$ XAF (82.9 €). The red line corresponds to the average fallow period $\tau = 37$ days, which yields the maximal profit $R = 52000$ XAF (79.3 €) and corresponds to the optimal constant fallow deployment. Parameter values are given in Tables 1 and 3.

All these solutions rely on the planting of a healthy vitroplant at the beginning of each cropping season. Vitroplants may not be readily available or their cost may be higher than the value retained in this case study. This motivates the next section.

V A MIXED DEPLOYMENT STRATEGY: WHEN AND HOW TO FALLOW

In this section, we analyse whether it is preferable to deploy a fallow after each cropping season, and therefore always rely on healthy vitroplants, or to let banana plants reproduce naturally.

5.1 Mixed strategies

In mixed strategies, the plant reproduces naturally during several seasons. After these successive seasons, a fallow is implemented. Following this fallow, the reproduction necessarily relies

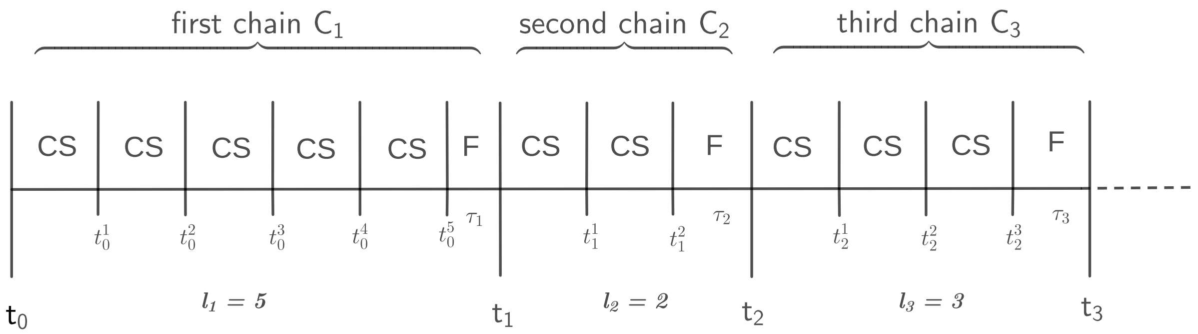

Figure 3: Illustration of the first three chains of a mixed strategy. Each chain C_i contains l_i cropping seasons (CS) and one fallow (F). Cropping seasons have a fixed duration (D) but fallow durations τ_i may vary.

on planting a healthy vitroplant. We name *chain*[1] the set of successive cropping seasons and the single fallow that follows.

Let us denote by;

1. C_i the i-th chain;
2. t_i the starting point of chain $C_{(i+1)}$;
3. t_i^j the starting point of the $(j+1)$-th season within chain $C_{(i+1)}$;
4. l_i the number of cropping seasons within chain $C_{(i)}$, defining the *size of the chain*;
5. τ_i the fallow duration of chain C_i, which follows the l_i cropping seasons;
6. T_i the duration of chain C_i.

Hence, cropping season j within chain C_i holds on the interval $(t_{i-1}^{j-1}, t_{i-1}^j]$.

Remark V.1:
$t_i^j = t_i + jD$, for all $j = 1, \dots, l_i - 1$ and $T_i = l_i D + \tau_i$.

Remark V.2:
A chain depends on its size l_i and its fallow duration τ_i, $C_i \equiv C_i(l_i, \tau_i)$.

A mixed strategy consists in a succession of chains and is illustrated in Figure 3.

5.2 Optimization problem

According to the definitions in Section 4.1.1, we define the profit of one cropping chain C_i as follows:

$$R(C_i) = R(l_i, \tau_i) = -c + \sum_{j=1}^{l_i} \int_{t_{i-1}^{j-1}}^{t_{i-1}^{j}} mS(t)dt. \tag{8}$$

Hence, the profit of $n+1$ chains $C_0, C_1, \dots, C_n$ is given by:

$$R(C_0, C_1, \dots, C_n) = R\big((l_i, \tau_i)_{i=0,\dots,n}\big) = \sum_{i=0}^{n} R(l_i, \tau_i). \tag{9}$$

---

[1] We could have called it *cycle*, but in the banana farming literature, the word *cycle* more commonly designates the growth time of a single banana plant from the time it is a viable sucker until the time it dies, in a context of natural reproduction.

On a finite time horizon T_{max}, the (l_i, τ_i) are such that $\sum_{i=0}^{n}(l_iD + \tau_i) \leq T_{max}$. With this condition, R admits a maximum according to the same arguments as in Tankam-Chedjou *et al.* (2021). If we name $\mathbb{A}^n$ the set of $(l_i, \tau_i)_{i=0,\dots,n}$ in $\mathbb{N}^* \times \mathbb{R}^*$, and $\mathcal{A}$ the reunion of $\mathbb{A}^n$, $n \geq 0$, then we state the general optimization problem as follows:

Problem V.1:
Find the optimal sequence $(l_i^*, \tau_i^*)_{i=0,\dots,n} \in \mathcal{A}$ of chain sizes and fallow durations that maximizes R defined in equation (9) on a finite time horizon T_{max}.

Problem V.1 admits a solution, but determining an optimal deployment strategy without any constraint is not obvious. Therefore, we concentrate on solving the problem on the case of fixed-size chains, with either constant or varying fallows.

5.3 Optimization with fixed-size chains and constant fallow

This subsection deals with the solution of Problem V.1 with fixed-size chains of size l when fallow durations are set to a constant value τ. Hence, mixed deployment strategies consist of a succession of identical chains.

5.3.1 Resolution

The maximal chain size l_{max} corresponds to a cropping strategy in which fallow periods are never deployed over T_{max}. Hence we have $l_{max} = \left\lfloor \frac{T_{max}}{D} \right\rfloor$.

Given a chain size $l \in \{1, \dots, l_{max}\}$ and a fallow duration τ, the number of complete chains that fit within the time horizon T_{max} is given by:

$$N \equiv N(l, \tau) = \left\lfloor \frac{T_{max} + \tau}{lD + \tau} \right\rfloor, \tag{10}$$

with the last chain allowed to have no fallow period.

Example V.1:
Let $T_{max} = 4000$ days and $D = 330$ days as in Table 1. The number of chains of size $l = 3$ and fallow duration $\tau = 10$ days is given by:

$$N(3, 10) = \left\lfloor \frac{4000 + 10}{3 * 330 + 10} \right\rfloor = 4.$$

If $\tau = 12$ days, still $N = 4$ both the 4^{th} chain ends with a 4-day fallow.

N is bounded as follows:

$$1 \leq N(l, \tau) \leq N(1, 0) = \left\lfloor \frac{T_{max}}{D} \right\rfloor. \tag{11}$$

If $T_{max} - (lD + \tau)N > D$, then an incomplete chain, i.e. a chain with less than l cropping seasons, can be introduced at the end of the complete chains. Formally, let $M = T_{max} - (lD + \tau)N$. If $M > D$ then let $p = \left\lfloor \frac{M}{D} \right\rfloor$. On can deploy an additional chain of size p and write profit (9) in this particular framework as follows:

$$R(l, \tau) = -c(N + 1) + m \sum_{i=1}^{N} \sum_{j=1}^{l} \int_{t_i^{j-1}}^{t_i^j} S(t)dt + m \sum_{j=1}^{p} \int_{t_N^{j-1}}^{t_N^j} S(t)dt, \tag{12}$$

where $N = N(l,\tau)$.

The profit $R(l,\tau)$ has a maximum for $(l,\tau) \in \Omega = \{1,\ldots,l_{max}\} \times [0, T_{max} - (l_{max}+1)D]$.

The optimization problem with fixed-size chains and constant fallow can therefore be written as follows:

Problem V.2:
Find $(l^*,\tau^*) \in \Omega$ such that $R(l^*,\tau^*) = \max_{(l,\tau)\in\Omega} Y(l,\tau)$, with $R(l,\tau)$ defined in equation (12).

Since the set of values of l is countable, we seek the solution τ^* of Problem (V.2) for each $l \in \{1,\ldots,l_{max}\}$ and compare them.

Remark V.3:
If $l = l_{max}$, there can be only one chain and the solution is trivial.

Remark V.4:
The solution is highly likely to be unique. If not, we could choose the solution that has the highest total fallow duration $\tau N(l,\tau)$ [2]. Different tie-break rules could be defined, depending on agricultural needs.

5.3.2 A case study

We solved Problem V.2 numerically using parameter values in Tables 1 and 3. Table 4 summarizes the optimal fallow durations for all possible chain sizes l over the time horizon $T_{max} = 4000$, and the yields that they generate. The optimum is obtained for $l^* = 1$, meaning that the chains consist of one cropping season followed by a fallow period. The optimal fallow duration obtained is $\tau^* = 37$ days and it generates a profit of 52,000 XAF (79.3 €). It corresponds to the optimum obtained with systematic and constant fallows.

Chain size l	Optimal fallow duration τ^*	Optimal number of complete chains N^*	Max number of complete chains	Number of cropping seasons of the incomplete chain p^*	Profit(XAF)
1	**37**	**11**	**12**	**0**	**52,000**
2	175	5	6	0	47,550
3	233	3	4	1	46,400
4	350	2	3	2	43,020
5	700	2	2	0	42,105
6	370	1	2	5	42,240
7	370	1	1	4	42,690
8	370	1	1	3	39,035
9	370	1	1	2	37,830
10	40	1	1	2	35,150
11	40	1	1	1	38,180
12	0	1	1	0	34,960

Table 4: Optimal fallow durations and generated profits for different chain sizes obtained for mixed deployment strategies with fixed-size chains and constant fallows. Parameters are found in Tables 1 and 3. The line in bold print indicates the overall optimum, obtained here for chains of size 1.

Several conclusions can be drawn from Table 4:

---

[2] The longer the fallow, the fewer crops are planted, thus reducing the cropping effort

1. The most profitable deployment is obtained for chains of size 1. This means that the cost of the vitroplant that could be saved by adopting vegetative reproduction is not sufficient to compensate for the loss of yield due to the infestation.
2. The optimal chains of size 6 are more profitable than the optimal chains of size 5, although the infestation is likely to get higher with 6 successive cropping seasons. This is because the former allows one more season (11) than the latter (10). However, the optimal chain of size 7, which allows the same number of cropping seasons (11), gives a better yield although it has more successive cropping seasons. In the same way, the optimal chain of size 11 gives a better yield than the ones of size 10.
3. The previous cases aside, increasing the chain size decreases the profit. This partly depends on the cost of the vitroplant. If we increase this cost tenfold, such that its value becomes $c = 2300$ XAF, we obtain the results depicted in Table 5. In this case, the profit reaches its optimal value R = 38550 XAF for a single chain of size $l = 7$, a single fallow period of duration $\tau = 370$ days, and a 4-season incomplete chain, in stark contrast with the previous case.

Chain size l	Optimal fallow duration τ^*	Optimal number of complete chains N^*	Max number of complete chains	Number of cropping seasons of the incomplete chain p^*	Profit (XAF)
1	37	11	12	0	29,230
2	175	5	6	0	37,200
3	233	3	4	1	38,120
4	350	2	3	2	36,810
5	700	2	2	0	37,965
6	370	1	2	5	38,100
7	**370**	**1**	**1**	**4**	**38,550**
8	370	1	1	3	34,875
9	40	1	1	3	33,860
10	40	1	1	2	31,010
11	40	1	1	1	34,040
12	0	1	1	0	32,890

Table 5: Optimal fallow durations and profits obtained for different chain sizes obtained for mixed deployment strategies with fixed-size chains and constant fallow. Parameters are found in Tables 1 and 3 except the vitroplant cost $c = 2300$ XAF. The line in bold print indicates the overall optimum, obtained here for chains of size 7.

5.4 Optimization with fixed-size chains and varying fallows

In this subsection, chains still have a constant size, but fallow durations vary. To simplify matters, rather than seeking for an optimal fixed-size chain, we aim at optimizing the fallow distribution, based on the optimal chains obtained in Subsection 5.3 with constant fallows.

5.4.1 Resolution

For a chain of size l, if N is the number of complete chains of size l and p the number of complete cropping seasons of the incomplete chain, then we look for a distribution $(\tau_i)_{i=1,\dots,N}$ of fallow periods such that:

$$\sum_{i=1}^{N} \tau_i = T_{max} - (NlD + pD), \tag{13}$$

which means that the last harvest occurs at T_{max}, with the last chain possibly being incomplete.

Let us define the simplex:

$$A_l^{N,p} \equiv \{(\tau_i)_{i=1,\dots,N} \subset \mathbb{R}^+ : \sum_{i=1}^{N} \tau_i = T_{max} - (klD + pD)\} \tag{14}$$

We define the profit for N chains of size l with an incomplete chain of size p, namely the profit of $(\tau_i)_{i=1,\dots,N}$ on $A_l^{N,p}$, as follows:

$$R_l^p(\tau_0, \dots, \tau_{N-1}) = -(N+1)c + \sum_{i=1}^{N} \sum_{j=0}^{l-1} \int_{t_i^j}^{t_i^{j+1}} mS(t)dt + \sum_{j=0}^{p-1} \int_{t_N^j}^{t_N^{j+1}} mS(t)dt. \tag{15}$$

The optimization problem we want to solve is the following.

Problem V.3:
Given $l \in \{1, \dots, l_{max}\}$, $p^* < l$, and $N^* > 0$ such that $T_{max} - (N^* lD + p^* D) \geq 0$, find $\vec{\tau}^* = (\tau_i^*)_{i=1,\dots,N} \in A_l^{N^*,p^*}$ such that

$$R_l^{p^*}(\vec{\tau}^*) = \max_{\vec{\tau} \in A_l^{N^*,p}} R_l^{p^*}(\vec{\tau})$$

,

where N^* and p^* are the optimal values obtained solving Problem V.2 with l fixed.

After having determined the solution with constant fallow durations τ^*, we capture the values of l, N^* and p^* from this solution. We then find the optimal fallow distribution with N^* fallow periods, chains of size l and a last chain of size p^* by running an adaptive random search algorithm (see Appendix B) on the simplex $A_l^{N^*,p^*}$.

5.4.2 *A case study*

We solve Problem V.3 numerically, using parameters in Table 1 and 3. We find the optimum for each $l \in \{1, \dots, l_{max}\}$ in order to perform comparisons. The optimum is obtained for $l^* = 1$. It corresponds to the solution obtained with systematic fallow deployment represented in Figure 2(a). Figure 4 gives a visual representation of this optimal solution. Table 6 summarizes the optimal distributions of fallow durations for all possible chain sizes and the profits that they generate.

Several conclusions can be drawn from Table 6:

1. As in the previous subsection, the most profitable deployment is obtained for chains of size 1. It corresponds to 11 cropping seasons, whereas the time horizon can span up to 12 cropping seasons.

Chain size l	Optimal fallow distribution τ^*	Optimal number of complete chains N^*	Number of cropping seasons of the incomplete chain p^*	Profit (XAF)
1	**(192, 81, 14, 39, 42, 0, 2, 0, 0, 0)**	**11**	**0**	**54,530**
2	(664, 0, 0, 0, 36)	5	0	47,615
3	(699, 0, 1)	3	1	46,625
4	(698, 2)	2	2	43,075
5	(610, 90)	2	0	42,105
6	(370)	1	5	42,240
7	(370)	1	4	42,690
8	(370)	1	3	39,035
9	(370)	1	2	37,830
10	(40)	1	2	35,150
11	(40)	1	1	38,180
12	(0)	1	0	34,960

Table 6: Optimal fallow duration distributions and profits obtained for different chain sizes for the mixed deployment strategy with fixed-size chains and varying fallow. The line in bold print indicates the overall optimum, obtained here for chains of size 1.

2. Table 7 gives the optimal fallow distributions and profits for all possible chain sizes when we increase the cost of vitroplants tenfold. The optima are obtained for the same distributions as in Table 6, but the profits are lower due to the higher vitroplant cost. The optimal deployment is obtained for 3 complete chains of size 3, whereas it is obtained for chains of size 7 when fallows are constant, as shown in Table 5. The optimal deployment with variable fallows allows for a very long fallow period (699 days) early on, which drastically reduces the nematode infestation. Figure 5 gives a visual representation of this optimal solution.
3. For the longer chain sizes ($l \geq 6$), which only allow 1 complete chain and hence 1 fallow period, results with fixed (Tables 4 and 5) and varying fallows (Tables 6 and 7) are identical in terms of optimal fallow duration and profit.

Chain size l	Optimal fallow distribution τ^*	Optimal number of complete chains N^*	Number of cropping seasons of the incomplete chain p^*	Profit (XAF)
1	(192, 81, 14, 39 42, 0, 2, 0, 0, 0)	11	0	31,760
2	(383, 274, 0, 43, 0)	5	0	37,265
3	**(699, 0, 1)**	**3**	**1**	**38,845**
4	(698, 2)	2	2	36,865
5	(610, 90)	2	0	37,965
6	(370)	1	5	38,100
7	(370)	1	4	38,550
8	(370)	1	3	34,895
9	(370)	1	2	33,690
10	(40)	1	2	31,010
11	(40)	1	1	34,040
12	(0)	1	0	32,890

Table 7: Optimal fallow durations and yields obtained for different chain sizes in the mixed control strategy with fixed-size chains and varying fallow when the cost of a healthy vitroplant is $c = 2300$ XAF. The line in bold print indicates the overall optimum, obtained here for chains of size 3.

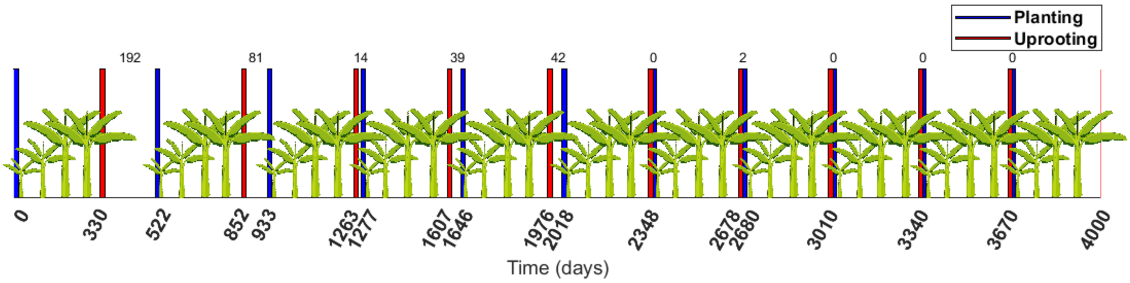

Figure 4: Visual representation of the optimal mixed deployment strategy with fixed-size chains and variable fallows. The optimum is obtained for chains of size 1 and the fallow distribution (192, 81, 14, 39, 42, 0, 2, 0, 0, 0). Parameters are found in Tables 1 and 3. The blue bars correspond to the planting of nematode-free vitroplant while the red bars correspond to the uprooting of plants after the harvest of the fruit bunch. The filled spaces over the course of time correspond to banana cropping seasons while the white spaces correspond to fallows whose durations are indicated at the top. Some fallows last 0 days and in these cases, the old plant is still uprooted and a nematode-free vitroplant is planted.

VI CONCLUSION

In subsections 5.3 and 5.4, we have seen that the optimal solutions with fixed-size chains are obtained with chains of size 1. This is because with larger chains, the infestation quickly becomes very high, which significantly reduces the yield. We have thus shown that the gain obtained by saving the cost of vitroplants when the seasons are allowed to chain by vegetative reproduction is not significant enough to compensate for the profit loss due to a higher infestation. We analysed nevertheless the solutions with different chain sizes, which showed profit losses of at least 8.56% compared to the optimal solution (size 1 chains). However, the conclusions changed when we increased the price of the vitroplant tenfold because the gain was much higher. In such case, the optima were found for chains of size 7 for constant fallows (Table 5) and chains of size 3 for variable fallows (Table 7).

The result of this optimization might be different if we admit different chain sizes from one chain to another. In this case, the size of the chains and the duration of the fallow periods must be optimized dynamically. Controlling chain sizes, which are necessarily integer values, could give rise to combinatorial problems. Several perspectives therefore emerge from this first approach to mixed deployment:

- We could control both the fallow durations and the size of the chains, so that the strategy decides at the end of each season, whether to let the plant reproduce or deploy a fallow (possibly of null duration), and in the latter case, how long a fallow. This amounts to finding the general solution to Problem V.1. Enumerating all the possible distributions $(l_i)_i$ of chain sizes and optimizing these distributions is not feasible over long time horizons as the number of distributions can explode very quickly. Also, it depends on the distribution of fallow periods. It is therefore necessary to optimize both simultaneously.
- When the seasons follow one another without uprooting, the infestation increases significantly, which has the effect of bringing the root biomass to very low levels (see Tankam-Chedjou *et al.* (2020), Fig.7). A low level of root biomass, which seems easy to obtain in this model, could lead to the fall of the plant [Blake (1972); Stover (1972)]. Moreover, banana suckers have a critical minimum level of root biomass to insure their survival [Serrano (2003)]. We could model the fall of plants by introducing an Allee effect in root growth, so that below this critical level the fresh root biomass would tend to perish.

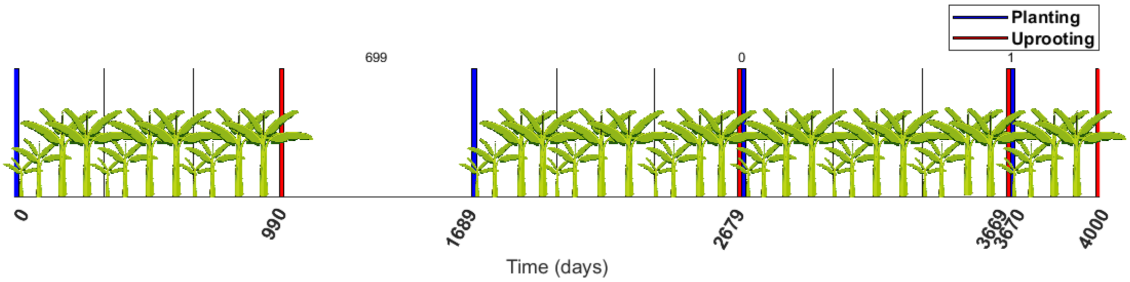

Figure 5: Visual representation of the optimal mixed deployment strategy with fixed-size chains and variable fallows. The optimum is obtained for chains of size 3 and the fallow distribution (699, 0, 1). Parameters are found in Tables 1 and 3 except the vitroplant cost $c = 2300$ XAF. The blue bars correspond to the planting of nematode-free vitroplant while the red bars correspond to the uprooting of plants at the end of the chain. The filled spaces over the course of time correspond to banana cropping seasons while the white spaces correspond to fallows whose durations are indicated at the top. In this strategy, a single 370-day long fallow is deployed.

The key input parameters of our optimization are the time horizon T_{max} and the initial soil infestation P_0. Hence, in order to apply our strategy in an operational context, the soil infestation has to be measured. Counting free-living soilborne nematodes is not an easy task but some methods are often adopted like the quantitative estimate of nematodes in small soil samples or geostatistical analysis [Minderman (1956); Webster and Boag (1992)]. After these measurements, and provided that the model parameters are well-calibrated, our optimization algorithm describes when to plant and when to leave the soil bare to have the best economic returns by the horizon T_{max}. Also, before applying such strategies in the field, agricultural constraints should be taken into consideration in our optimization problem. For instance, fallow durations would certainly need to be upper-bounded, as long periods without crops also mean long periods with reduced earnings. These strategies would probably meet with low acceptability among banana producers, who might prefer using nematicides. Fallow durations could also be lower-bounded, so as to implement crop rotations between banana plants and other crops that could provide an extra income. This approach could be extended to other soil-borne pests that are obligate root parasites, as fallow deployment would similarly impact their development. The seasonal model would need to be adapted to take into account the pest population dynamics and its interactions with the plant host.

References

Araya M., Centeno M. (1995). Recuperacion de Radopholus similis, Helicotylenchus spp., Meloidogyne spp. y Pratylenchus spp. de raiz funcional, no funcional y combinada de banano (Musa AAA). *Corbana: revista de la Corporacioón Bananera Nacional (Costa Rica) 20*, 11–16.

Bahar N. H., Lo M., Sanjaya M., Van Vianen J., Alexander P., Ickowitz A., Sunderland T. (2020). Meeting the food security challenge for nine billion people in 2050: What impact on forests? *Global Environmental Change 62*, 102056.

Beugnon M., Champion J. (1966). Etude sur les racines du bananier. *Fruits 21*(7), 309–327.

Blake C. D. (1966). The histological changes in banana roots caused by radopholus similis and helicotylenchus multicinctus. *Nematologica 12*, 129–137.

Blake C. D. (1972). *Nematode diseases of banana plantations*. London, UK: Academic Press.

Chabrier C., Mauléon H., Bertrand P., Lassoudière A., Quénéhervé P. (2005). Banane antillaise, les systèmes de culture évoluent: en Martinique, méthodes alternatives pour réduire l'utilisation des nématicides et insecticides en bananeraies. *Phytoma – La défense des végétaux 584*, 12–16.

Chabrier C., Quénéhervé P. (2003). Control of the burrowing nematode (*Radopholus similis* Cobb) on banana: impact of the banana field destruction method on the efficiency of the following fallow. *Crop protection 22*(1), 121–127. doi:10.1016/S0261-2194(02)00121-7.

Chabrier C., Tixier P., Duyck P.-F., Cabidoche Y.-M., Quénéhervé P. (2010). Survival of the burrowing nematode *Radopholus similis* (Cobb) Thorne without food: Why do males survive so long? *Applied Soil Ecology 45*(2), 85–91. doi:10.1016/j.apsoil.2010.02.005.

Duncan L. W., Kaplan D. T., Noling J. W. (1990). Maintaining barriers to the spread of *Radopholus citrophilus* in Florida citrus orchards. *Nematropica 20*(1), 71–87. URL: `https://journals.flvc.org/nematropica/article/view/63977`.

Eckstein K., Robinson J. C. (1999). The influence of the mother plant on sucker growth, development and photosynthesis in banana (Musa AAA; Dwarf Cavendish). *The Journal of Horticultural Science and Biotechnology 74*(3), 347–350. doi:10.17660/ActaHortic.2000.531.23.

Efanden C., Kwa M., Temple L., Foundjem D. (2005, 31 octobre – O3 novembre). Production de plantain dans la zone périurbaine de Yaoundé : identification des contraintes et incidences sur la localisation de la zone d'approvisionnement et stratégie d'intervention. In L. Parrot, A. Njoya, L. Temple, F. Assogba-Komlan, R. Kahane, M. Ba Diao, and M. Havard (Eds.), *Actes de l'atelier international "Agricultures et développement urbain en Afrique de l'ouest et du centre"*, Yaoundé, Cameroun, pp. 109–113.

Fargette M., Quénéhervé P. (1988). Populations of nematodes in soils under banana, cv. Poyo, in the Ivory Coast. The nematofauna occurring in the banana producing areas. *Revue de Nématologie 51*(2), 239–244.

Food and Agriculture Organization of the United Nations (FAO) (2020). *Banana facts and figures*. Accessed 24 March 2020. URL: `http://www.fao.org/economic/est/est-commodities/bananas/bananafacts/en/`.

Gilligan C. A. (1990). Mathematical modeling and analysis of soilborne pathogens. In J. Kranz (Ed.), *Epidemics of Plant Diseases: Mathematical Analysis and Modeling* (Second ed.), Volume 13 of *Ecological Studies*, pp. 96–142. Berlin, Heidelberg: Springer. doi:10.1007/978-3-642-75398-5_4.

Gilligan C. A. (1995). Modelling soil-borne plant pathogens: reaction-diffusion models. *Canadian Journal of Plant Pathology 17*(2), 96–108. doi:10.1080/07060669509500700.

Gowen S. R. (1997). Chemical control of nematodes: efficiency and side-effects. In M. A. Maqbool and B. Kerry (Eds.), *Plant nematode problems and their control in the Near East region*, Volume 144 of *Plant Production and Protection Paper*, pp. 59–65. FAO. URL: `http://www.fao.org/3/V9978E/v9978e00.htm`.

Gubbins S., Gilligan C. A., Kleczkowski A. (2000). Population dynamics of plantparasite interactions: Thresholds for invasion. *Theoretical Population Biology 57*(3), 219 – 233. doi:10.1006/tpbi.1999.1441.

Hugon R., Picard H. (1988). Relations spatiales entre taches et nécroses racinaires et nématodes endoparasites chez le bananier. *Fruits 43*(9), 491–498.

Kaplan D. T., Opperman C. H. (2000). Reproductive strategies and karyotype of the burrowing nematode, *Radopholus similis*. *Journal of Nematology 32*(2), 126–133. URL: `https://journals.flvc.org/jon/article/view/67136`.

Liu P. (2008). Certification in the value chain for fresh fruits: The example of banana industry. FAO commodity studies 4. URL: `http://www.fao.org/3/i0529e/i0529e00.htm`.

Loridat P. (1989). Etude de la microflore fongique et des nématodes associés aux nécroses de l'appareil souterrain du bananier en Martinique. mise en évidence du pouvoir pathogène du genre *Cylindrocladium*. *Fruits 44*(11), 587–598.

Madden L. V., Van Den Bosch F. (2002). A population-dynamics approach to assess the threat of plant pathogens as biological weapons against annual crops: using a coupled differential-equation model, we show the conditions necessary for long-term persistence of a plant disease after a pathogenic microorganism is introduced into a susceptible annual crop. *BioScience 52*(1), 65–74. doi:10.1641/0006-3568(2002)052[0065:APDATA]2.0.CO;2.

Mailleret L., Castel M., Montarry M., Hamelin F. (2011). From elaborate to compact seasonal plant epidemic models and back: Is competitive exclusion in the details? *Theoretical Ecology 5*, 311–324. doi:10.1007/s12080-011-0126-0.

Marin D. H., Sutton T. B., Barker K. R. (1998). Dissemination of bananas in Latin America and the Caribbean and its relationship to the occurrence of *Radophouls similis*. *Plant Disease 82*(9), 964–974.

doi:10.1094/PDIS.1998.82.9.964.

Minderman G. (1956). New techniques for counting and isolating free living nematodes from small soil samples and from oak forest litter. *Nematologica 1*(3), 216 – 226. URL: `https://brill.com/view/journals/nema/1/3/article-p216_6.xml`, doi:10.1163/187529256X00069.

Moreau B., Le Bourdelles J. (1963). Etude du système racinaire du bananier Gros Michel en Equateur. *Fruits 18*(2), 71–74.

Namaganda J. M., Kashaija I. N., Maslen R. (2002). Host status of the common weeds of banana establishments to banana nematodes in Uganda. *International Journal of Fundamental and Applied Nematological Research 4*(2), 271. doi:10.5829/idosi.ajps.2018.11.1.01.10.

Ngo-Samnick E. L. (2011). *Production améliorée du bananier plantain*. Centre Technique de Coopration Agricole et Rurale (CTA) & Ingnieurs sans Frontires (ISF) Cameroun. Collection PRO-AGRO. URL: `https://hdl.handle.net/10568/75517`.

Nilusmas S., Mercat M., Perrot T., Djian-Caporalino C., Castagnone-Sereno P., Touzeau S., Calcagno V., Mailleret L. (2020). Multi-seasonal modelling of plant-nematode interactions reveals efficient plant resistance deployment strategies. *Evolutionary Applications 00*, 1–16. doi:10.1111/eva.12989.

Plowright R., Dusabe J., Coyne D., Speijer P. (2013, 01). Analysis of the pathogenic variability and genetic diversity of the plant-parasitic nematode Radopholus similis on bananas. *Nematology 15*, 41–56. doi:10.1163/156854112X643914.

Quénéhervé P. (1989). Population of nematodes in soil under banana, cv. Poyo, in the Ivory Coast. 5. Screening of nematicides and horticultural results. *Rev. Nématol. 14*, 231–249.

Robinson J. C., Saúco V. G. (2010). *Bananas and plantains* (Second ed.), Volume 19 of *Crop Production Science in Horticulture*. CABI Publishing.

Sarah J.-L. (1986). Répartition spatiale des infestations racinaires de *radopholus similis* (COBB) en relation avec la croissance et le développement du bananier Poyo en Côte d'ivoire. *Fruits 41*, 427–435.

Sarah J.-L. (1993). Variabilité du pouvoir pathogène de *Radopholus similis* entre populations provenant de différentes zones de production du monde. *Infomusa (Ed. Française) 2*(2), 6.

Sarah J.-L., Lassoudière A., Guérout R. (1983). La jachère nue et l'immersion du sol: deux méthodes intéressantes de lutte integrée contre *Radopholus similis* (Cobb.) dans les bananeraies des sols tourbeux de Côte d'Ivoire. *Fruits 38*(1), 35–42.

Serrano E. (2003). Relationship between functional root content and banana yield in Costa Rica. In D. W. Turner and F. E. Rosales (Eds.), *Banana root system: towards a better understanding for its productive management*, pp. 25–34. Proceedings of an international symposium held in San José, Costa Rica, 3-5 November 2003.

Stover R. H. (1972). *Banana, plantain and abaca diseases*. Kew, UK: Commonwealth Mycological Institute.

Tankam-Chedjou I., Grognard F., Tewa J. J., Touzeau S. (2021). Optimal and sustainable management of a soilborne banana pest. *Applied Mathematics and Computation 397*, 125883. doi:https://doi.org/10.1016/j.amc.2020.125883.

Tankam-Chedjou I., Touzeau S., Mailleret L., Tewa J. J., Grognard F. (2020). Modelling and control of a banana soilborne pest in a multi-seasonal framework. *Mathematical Biosciences 322*, 108324. doi:10.1016/j.mbs.2020.108324.

Taylor C. R., Rodrìguez-Kábana R. (1999). Optimal rotation of peanuts and cotton to manage soil-borne organisms. *Agricultural Systems 61*(1), 57–68. doi:10.1016/S0308-521X(99)00034-7.

Temple L., Kwa M., Fogain R., Pefoura A. M. (2006). Participatory determinants of innovation and their impact on plantain production systems in cameroon. *International Journal of Agricultural Sustainability 4*(3), 233–243.

Thompson R. N., Jalava K., Obolski U. (2019). Sustained transmission of ebola in new locations: more likely than previously thought. *The Lancet Infectious Diseases 19*(10), 1058–1059. doi:10.1016/S1473-3099(19)30483-9.

Van den Berg W., Rossing W. (2005). Generalized linear dynamics of a plant-parasitic nematode population and the economic evaluation of crop rotations. *Journal of Nematology 37*(1), 55–65. URL: `https://journals.flvc.org/jon/article/view/67536`.

Van Den Berg W., Rossing W. A. H., Grasman J. (2006). Contest and scramble competition and the carry-over effect in Globodera spp. in potato-based crop rotations using an extended Ricker model. *Journal of Nematology 38*(2), 210–220. URL: `https://journals.flvc.org/jon/article/view/67645`.

Van den Berg W., Vos J., Grasman J. (2012). Multimodel inference for the prediction of disease symptoms and yield loss of potato in a two-year crop rotation experiment. *International Journal of Agronomy 2012*, 438906. doi:10.1155/2012/438906.

Van Weerdt L. G. (1960). Studies on the biology of *Radopholus similis* (Cobb, 1893) Thorne, 1949. Part III Embryology and post-embryonic development. *Nematologica 5*(1), 43–52. doi:10.1163/187529260X00244.

Webster R., Boag B. (1992). Geostatistical analysis of cyst nematodes in soil. *Journal of Soil Science 43*(3), 583–595. URL: `https://onlinelibrary.wiley.com/doi/abs/10.1111/j.1365-2389.1992.tb00162.x`, arXiv:https://onlinelibrary.wiley.com/doi/pdf/10.1111/j.1365-2389.1992.tb00162.x, doi:10.1111/j.1365-2389.1992.tb00162.x.

A PARAMETER CALIBRATION

Most of the parameters are set to realistic values obtained from experimental studies in the literature. However, some parameters cannot be easily measured. We remind the calibration measures taken in Tankam-Chedjou *et al.* (2020):

- The infestation rate β is chosen such that the nematode population in the soil remains marginal [Fargette and Quénéhervé (1988); Namaganda *et al.* (2002); Quénéhervé (1989); Sarah *et al.* (1983)].
- The root growth rate ρ is estimated such that $S(d) \simeq K$.
- The magnitude of the consumption rate a is evaluated from the size of a single nematode [Van Weerdt (1960)].
- The conversion rate of ingested root α and the half-saturation constant Δ are estimated to maintain a sensible population size.
- The proportion of roots forming the new sucker is chosen such that the proportion q of the maximum biomass K is close to the pest survival critical level.
- The proportion r of pests released in the soil after uprooting is set assuming that the uprooting is properly done.
- The initial root biomass corresponds to the sucker survival critical level [Serrano (2003)].

B ADAPTIVE RANDOM SEARCH ON THE SIMPLEX

The ARS algorithm, adapted to the n-simplex A^n, is described below. It aims at determining the optimal fallow distribution ARS$(n) = \vec{\tau}^{n,*} = (\tau_1^*, \ldots, \tau_n^*)$ that maximizes the Profit R defined in equation (6) for a given number of fallows n. It is also adaptable to simplexes $A_l^{N,p}$ defined in equation 14 to solve the problem V.3

(Initialization)

Step 1 – Start as the center of the simplex:

$$\vec{\tau}^{n,*} := [T_{max} - (n+1)D] \left(\frac{1}{n}, \ldots, \frac{1}{n} \right)$$

and initialize the standard deviation at the “size” of the simplex:
$\sigma^* = \sigma^0 := T_{max} - (n+1)D.$

(Variance-selection)

It aims at finding the best standard deviation σ^*.

Step 2 – 5 decreasing standard deviations $\sigma^{i \in \{1,\ldots,5\}} < \sigma^0$ are chosen. For each standard deviation, $2 \times n^2$ fallow distributions are drawn randomly in the simplex and their profit is evaluated. The best standard deviation, selected for the next step, is the one corresponding to the highest profit.

```
$\vec{\tau}_{sel} := \vec{\tau}^{n,*}$
for $i$ := 1 to 5 do
    $\sigma^i := 0.3 \times \sigma^{i-1}$
    for $j$ := 1 to $2 \times n^2$ do
        Draw $\vec{d^j}$ (cf. below)
        Draw $r^j \sim \mathcal{N}(0, \sigma^i)$
        $\vec{\tau}^j := \vec{\tau}_{sel} + r^j \vec{d^j}$
        while $\vec{\tau}^j$ is outside of the simplex do
            Draw $r^j \sim \mathcal{N}(0, \sigma^i)$
            $\vec{\tau}^j := \vec{\tau}_{sel} + r^j \vec{d^j}$
        end
        if $R(\vec{\tau}^j) > R(\vec{\tau}^{n,*})$ then
            $\vec{\tau}^{n,*} := \vec{\tau}^j$ and $\sigma^* := \sigma^i$
        end
    end
end
```

$\vec{d^j}$ draw:

1. $\vec{d^j} \sim \mathcal{U}\big([0,1]^n\big)$;
2. project $\vec{d^j}$ on the hyperplane $H = \{(d_k) \in \mathbb{R}^n | \sum_{k=1}^n d_k = 0\}$;
3. normalize $\vec{d^j}$.

(Variance-exploitation)
It aims at finding the best fallow distribution $\vec{\tau}^{n,*}$.

Step 3 – $5 \times n^2$ fallow distributions are drawn randomly in the simplex, using the best standard deviation σ^* selected from the previous variance-selection phase, and their profit is evaluated. The best fallow distribution is the one with the highest yield.

```
for $j$ := 1 to $5 \times n^2$ do
    Draw $\vec{d^j}$ (cf. above)
    Draw $r^j \sim \mathcal{N}(0, \sigma^*)$
    $\vec{\tau}^j := \vec{\tau}^{n,*} + r^j \times \vec{d}$
    while $\vec{\tau}$ is outside of the simplex do
        Draw $r^j \sim \mathcal{N}(0, \sigma^*)$
        $\vec{\tau}^j := \vec{\tau}^{n,*} + r^j \vec{d^j}$
    end
    if $R(\vec{\tau}^j) > R(\vec{\tau}^{n,*})$ then
        $\vec{\tau}^{n,*} := \vec{\tau}^j$
    end
end
```

(Stopping criteria)
Steps 2 and 3 are repeated until one of the following stopping criteria is achieved:

- The smallest standard deviation σ^5 is used in more than 4 successive variance-exploitation phases.
- The optimum is not improved in more than 4 successive variance-exploitation phases.
- The yield is evaluated more than $100 \times n^2$ times.